Draft version December 12, 2014
Preprint typeset using LaTeX style emulateapj v. 04/17/13

RADIO SOURCES IN THE SERPENS SOUTH PROTOCLUSTER

Authors

ABSTRACT

We present 4.14 and 6.31 centimeter continuum observations of the Serpens South protocluster with the Karl G. Jansky Very Large Array in its C configuration. Our focus is a 4' x 4' area around the central filament ($\alpha = 18^{\rm h}30^{\rm m}05.00^{\rm s}, \delta = -02°02'30.0''$, J2000.0). We detect roughly 18 sources, 10 of which are probably protostellar in nature. We characterize the radio emission and put it in context with 2MASS, Spitzer and Herschel data from the region. We find new embedded protostars that have yet to be resolved at shorter wavelengths, and in some cases confirm compact centimeter emission in previously labeled starless cores. We compare our radio sources to the known centimeter vs. bolometric luminosity relationship. With our relatively short integration time and weak detection of many more possible radio sources, we speculate that longer, higher resolution radio measurements of the region would yield confident detections of many more radio protostars.

1. INTRODUCTION

Serpens South is a young stellar cluster that is a part of the broader Aquila Rift extinction feature. It lies south of the Serpens Main cloud, and is just West of the bright W40 HII region. Discovered in 2008 by Gutermuth et al. (2008) as a part of the Spitzer Space Telescope's Gould Belt Legacy survey, Serpens South has been found to harbor an unusually high ratio of Class I to Class II protostars, suggesting it is in a very early phase of cluster formation. Since its discovery, it has become the center of a wide range of scholarship. This has consisted of near, mid and far infrared mappings with Spitzer and Herschel tracing heated dust around protostars (Gutermuth et al. 2008; Bontemps et al. 2010), millimeter mappings with MAMBO on the IRAM 30-meter tracing cold dust (Maury et al. 2011), near infrared polarimetry revealing the importance of global magnetic fields in the cluster's formation history (Sugitani et al. 2011), molecular outflows studies (Nakamura et al. 2011; Teixeira et al. 2012), and a wealth of spectral line surveys probing filamentary infall (Kirk et al. 2013; Friesen et al. 2013; Tanaka et al. 2013; Fernández-López et al. 2014; Nakamura & Li 2014). X-ray studies of Serpens South have yet to be published. Presently only one radio study of Serpens South has been conducted, which used the VLA in its A configuration in 2011 (Ortiz-Leon et al. in prep). Beyond this study, further radio studies of Serpens South will be important in understanding the star formation process across the electromagnetic spectrum.

The VLA has been a proven tool in searching for and detecting radio emission around protostars since the early 1990s (e.g., Curiel et al. 1989; Anglada et al. 1998; Reipurth et al. 1999; Beltrán et al. 2001; Eiroa et al. 2005; Shirley et al. 2007; Rodríguez et al. 2010). Early radio studies of protostars found an excess of radio emission in comparison to the Lyman-Alpha continuum drop off expected from a normal ZAMS star. Theory and observations have best explained protostellar radio emission as having two components: thermal and non-thermal. Thermal radio emission is generally assumed to be free-free emission created from an HII region. High mass protostars have a high enough internal luminosity to support a compact or ultra-compact HII region, however, low mass protostars do not. HII regions surrounding low-mass protostars are created from thermal jets that shock the material surrounding the protostar. Non-thermal emission around low and high mass protostars is still not clearly understood; it is thought to come from gyrosynchrotron emission or possibly from jets that produce synchrotron emission in their tails.

1.1. *Distance to Serpens South*

The distances to Serpens South, W40 and the Serpens Main cloud are not agreed upon in the literature. When Serpens South was discovered in 2008, a distance of 260 pc ± 37 pc was adopted based on evidence that its LSR velocities matched LSR velocities of the Serpens Main cloud, which was then thought to be a part of the larger Aquila Rift extinction feature whose distance was estimated at 260 pc by Straižys et al. (2003). However, VLBA parallax measurements done in 2010 have established the distance to the Serpens Main cloud as 429 ± 2 pc (Dzib et al. 2011), meaning that Serpens Main is distinct from the the Aquila Rift if the latter is to have a distance of 260 pc.

Gutermuth et al. (2008) also argued that Serpens South lies in front of W40, claiming that it is seen in absorption against emission from W40. Therefore, we know Serpens Main is at 429 pc, and we know that Serpens South lies in front of W40. What we don't know are the absolute distances to both W40 or Serpens South. If we are to follow the initial LSR velocity analysis by Gutermuth et al. (2008), we would equate Serpens South to Serpens Main and say Serpens South lies at approximately 429 pc, while W40 lies further away. Indeed, recent radio and x-ray studies adopt a distance of 600 pc to W40, although they admit the distance is poorly constrained (Kuhn et al. 2010; Rodríguez et al. 2010). Here, we adopt a distance of 429 pc for Serpens South, although we comment on how a 260 pc distance estimate would change our analysis.

2. OBSERVATIONS

We observed Serpens South on July 2, 2013, for 1 hour with the EVLA in its C array configuration. The increased bandwidth of the EVLA allowed us to split

TABLE 1
EVLA Image Properties

Wavelength (cm)	Beam Size[a] (arcsec x arcsec)	Position Angle (degrees)	Image RMS (μJy beam^{-1})
6.31	4.8 x 3.9	13.4	11.1
4.14	3.2 x 2.5	12.7	8.5

[a] Images deconvolved with robust (Briggs) weighting, *robust*=0.5 (Briggs 1995).

our C band observation into two subbands centered at 4.75 GHz (6.31 cm) and 7.25 GHz (4.14 cm), with a bandwidth of 1.024 GHz for each subband. We focused on a 3.5 arcsec x 3.5 arcsec region around Serpens South's central filament, with a phase center positioned at α(J2000) = $18^{\rm h}30^{\rm m}05.00^{\rm s}, \delta$(J2000) = $-02°02'30.0''$. Gain calibrations were done by switching to J1804 + 0101 every 10 minutes during our hour-long observation. Figure 1 shows Serpens South at 350 micron and outlines our field of view.

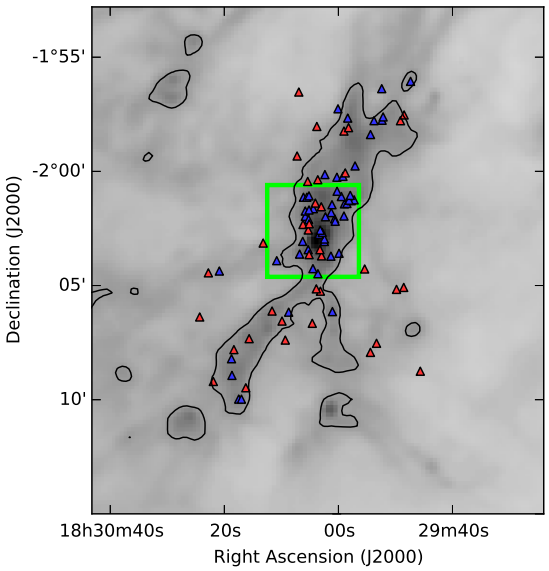

Fig. 1.— Herschel SPIRE 350 μm greyscale image of Serpens South. Blue and red triangles indicate Spitzer identified Class I and Class II protostars respectively. The green box indicates our region of interest with the EVLA.

We manually flagged, calibrated and imaged our data with standard procedures using Common Astronomy Software Applications (CASA) 4.1.0. We used J1331+305 (3C286) as a flux and bandpass calibrator, and J1804+0101 as a gain and phase calibrator ($S_{6.31\rm cm}$ = 0.70 ± 0.02 Jy, $S_{4.14\rm cm}$ = 0.66 ± 0.02 Jy). We deconvolved the Stokes I images with the Cotton-Schwab algorithm (Schwab 1984) using the CLEAN method (Högbom 1974; Clark 1980). We experimented with natural, robust and uniform weighting, and found the best compromise between noise level and source resolution with robust weighting, also known as Briggs weighting (Briggs 1995), with a *robust* parameter set to 0.5. The synthesized beam sizes and RMS values for our two images are detailed in Table 1. We also deconvolved the Stokes V images, but did not find any significant signal.

Observing Serpens South at radio wavelengths is difficult because of the extended and bright HII region W40 directly to the East, which adds to over-resolved flux and increases the RMS noise level in our images. In addition, our short integration time–45 minutes on source–left us with a less than desirable UV coverage at long UV distances. Long UV distance coverage is particularly important because we are trying to resolve point source emission. Further EVLA studies of Serpens South would benefit from extended array configurations and longer integration times.

3. RESULTS

3.1. *Radio Source Selection*

In choosing our sources, we restrict ourself to a circular region centered on our phase center and extending out to 50% of the primary beam strength. We choose our sources based on their strength in our 4.1 and 6.3 cm maps, their possible spatial alignment with infrared sources, and by referencing a source extracted sample using Sextractor (Bertin & Arnouts 1996). We were left with a total of 18 radio sources. We then ran source extractions on these spatial positions over the JHK bands of 2MASS, the four IRAC bands of Spitzer, the 24 μm MIPS band on Spitzer, and the 70 μm PACS band on Herschel. We used a 2 arcsecond maximum matching tolerance for these extractions. Apertures and adopted corrections are consistent with the HOPS survey.

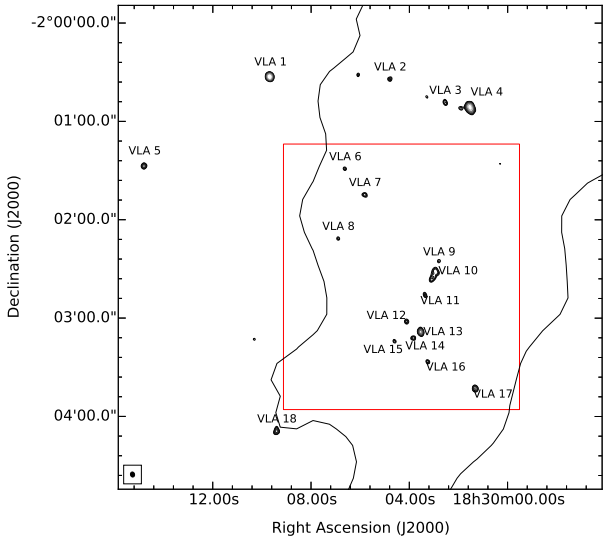

Fig. 2.— Serpens South radio continuum at 6.3 cm, focused in on green box from Figure 1. Radio contours start at 4σ and end at 50σ. The loose black contour is the same SPIRE 350 μm contour found in Figure 1.

Eight of our radio sources have at least one infrared source match from 1.25 μm to 70 μm, four of which spatially match Spitzer identified Class I/II protostars within 1 arcsecond. A total of ten out of our 18 sources have signs that indicate they are protostellar in nature. One of our radio sources matches a 1.2 mm source within 1 arcsecond identified by (Maury et al. 2011), which they state as starless. Here, we confirm compact radio emission with a rising spectral index indicative of mixed op-

TABLE 2
RADIO PROPERTIES OF VLA SOURCES

Source	RA[a] (J2000)	Decl.[a] (J2000)	$S^{\rm int}_{6.3{\rm cm}}$ [b] (μJy)	$S^{\rm peak}_{6.3{\rm cm}}$ (μJy beam^{-1})	$S^{\rm int}_{4.1{\rm cm}}$ (μJy)	$S^{\rm peak}_{4.1{\rm cm}}$ (μJy beam^{-1})	$\alpha^{\rm int}_{\rm radio}$	$\alpha^{\rm peak}_{\rm radio}$
VLA_1	18:30:09.68	-02:00:32.8	844 ± 8	794	749 ± 6	718	0.28 ± 0.01	0.24 ± 0.02
VLA_2	18:30:04.79	-02:00:34.1	87 ± 7	72	177 ± 7	138	-1.67 ± 0.09	-1.55 ± 0.14
VLA_3	18:30:02.55	-02:00:48.5	116 ± 10	87	140 ± 2	99	-0.46 ± 0.1	-0.3 ± 0.15
VLA_4	18:30:01.53	-02:00:51.6	946 ± 28	515	1663 ± 32	1178	-1.33 ± 0.04	-1.96 ± 0.02
VLA_5	18:30:14.79	-02:01:27.3	167 ± 10	173	106 ± 5	95	1.07 ± 0.08	1.41 ± 0.13
VLA_6	18:30:06.62	-02:01:28.9	33 ± 4	56	79 ± 7	61	-2.04 ± 0.16	-0.22 ± 0.23
VLA_7	18:30:05.81	-02:01:44.9	84 ± 7	63	48 ± 4	40	1.29 ± 0.13	1.08 ± 0.31
VLA_8	18:30:06.89	-02:02:11.5	50 ± 6	50	39 ± 3	46	0.55 ± 0.15	0.18 ± 0.29
VLA_9	18:30:02.80	-02:02:25.3	60 ± 1	44	66 ± 1	50	-0.22 ± 0.03	-0.31 ± 0.29
VLA_10	18:30:02.95	-02:02:32.2	260 ± 17	73	287 ± 6	119	-0.23 ± 0.07	-1.15 ± 0.15
VLA_11	18:30:03.36	-02:02:45.8	73 ± 4	58	38 ± 2	36	1.5 ± 0.09	1.14 ± 0.34
VLA_12	18:30:04.11	-02:03:02.1	79 ± 2	58	30 ± 2	24	2.31 ± 0.09	2.06 ± 0.48
VLA_13	18:30:03.54	-02:03:08.4	231 ± 3	227	186 ± 1	178	0.51 ± 0.02	0.58 ± 0.07
VLA_14	18:30:03.84	-02:03:12.2	83 ± 2	61	31 ± 0	37	2.29 ± 0.04	1.19 ± 0.33
VLA_15	18:30:04.60	-02:03:14.1	49 ± 4	51	68 ± 1	52	-0.74 ± 0.09	-0.08 ± 0.27
VLA_16	18:30:03.25	-02:03:26.6	55 ± 1	65	63 ± 2	58	-0.28 ± 0.04	0.27 ± 0.23
VLA_17	18:30:01.32	-02:03:42.9	161 ± 4	167	146 ± 3	135	0.22 ± 0.04	0.5 ± 0.1
VLA_18	18:30:09.40	-02:04:08.8	167 ± 10	134	170 ± 3	182	-0.04 ± 0.07	-0.71 ± 0.09

[a] Centers of 2D gaussian fits for sources in 4.1 cm map, quoted in J2000 coordinates.
[b] Flux values from images deconvolved with Briggs weighting, *robust*=0.5 (Briggs 1995).
[c] Spectral index of integrated flux from 6.3 to 4.1 cm, see section 3 for details on calculation.
[d] Spectral index of peak flux from 6.3 to 4.1 cm.
[e]

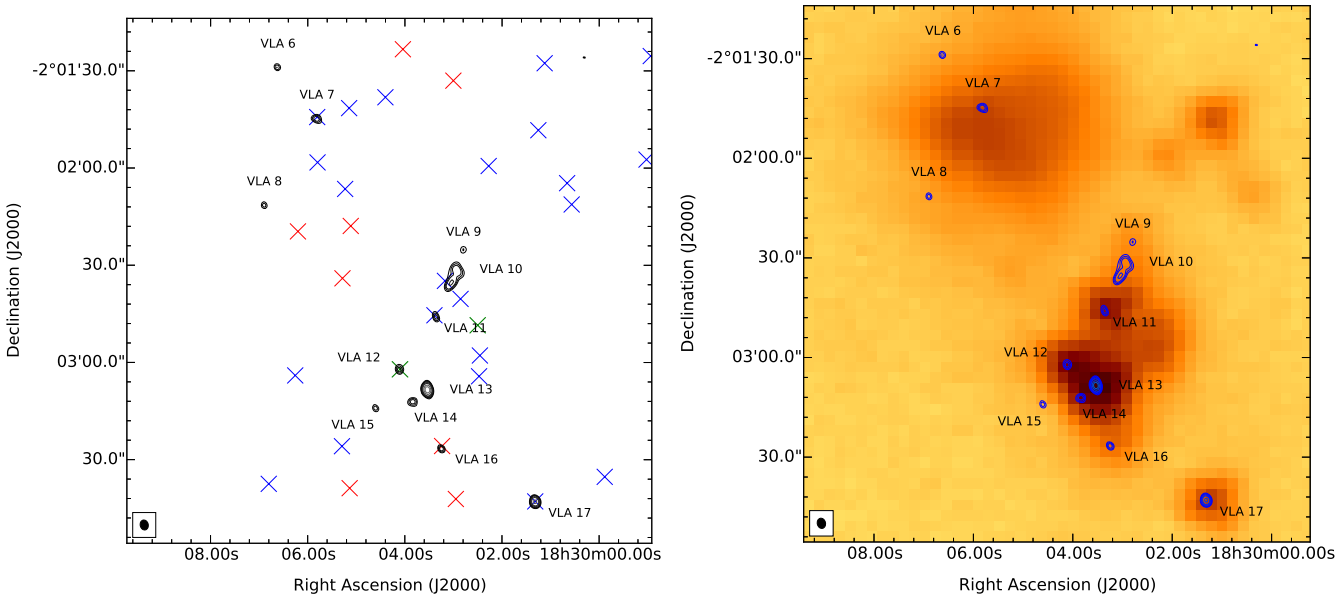

FIG. 3.— **Left**: Radio continuum of central filament at 6.3 cm, focused in on red box from Figure 2. Blue and red crosses correspond to Class I and II protostars identified by Spitzer (Gutermuth et al. 2008). Green crosses correspond to 1.2 mm dust peaks identified by IRAM (Maury et al. 2011). **Right**: Identical image as figure on the left, but the background color is PACS 70 μm image.

tically thin and thick free-free emission, which suggests the presence of a compact core.

We can calculate the number of random background sources we would expect to find in our images. We use the formulation found in Shirley et al. (2007), who draw from radio studies done by Fomalont et al. (1991). The density of random background radio sources above a flux limit of S μJy at 6 cm is given by $N(>S) = 0.42 \cdot (S/30\ \mu\text{Jy})^{-1.18}$ arcmin^{-2}. Therefore, the total number of sources with flux S greater than 50 μJy at 6 cm is 0.229 arcmin^{-2}. This leads to a 0.4% chance that a background source falls inside any one synthesized beam centered on a compact star, and gives us on average ∼9 background sources above 50 μJy within our 3.5' x 3.5' region of interest. This agrees with our analysis, as we find roughly 8 sources that are likely background sources.

3.2. *Radio Source Properties*

VLA 1 - 5 — VLA 1 is relatively isolated from the cluster, has very strong radio emission and has no known protostellar matches in the infrared. These alone would suggest an extragalactic classification, however, it has a slightly rising radio spectral index of 0.28 indicative of optically thin free-free emission. While galaxies are capable of producing free-free emission from large HII regions, non-thermal synchrotron emission with a steep negative spectral index generally dominates a galaxies' radio emission output. However, because VLA 1 does not spatially match any near or far infrared emission structures, we conclude it is extragalactic in nature.

Sources 2 through 4 seem to be extragalactic. They have no infrared or far-infrared matches and have steep negative radio spectral indices that suggests their emission is non-thermal synchrotron.

VLA 5 is isolated from the cluster and has no infrared or far-infrared matches, but has a strongly rising radio spectral index of 1.41 suggesting that it comes from optically thick free-free emission. Similar to VLA 1, we conclude that it is extragalactic.

4. DISCUSSION

4.1. *Protostars in the Central Filament*

Spitzer observations revealed dozens of Class I and II protostars spatially correlated to the central filament (Gutermuth et al. 2008). Herschel observations revealed colder clumps of dust corresponding to younger Class 0 protostars (Bontemps et al. 2010), however, with their poor spatial resolution they cannot reasonably resolve individual compact cores.

4.2. *$L_{infrared}$ and L_{bol} Relationship*

The internal luminosity $L_{\rm int}$ of a protostar is defined as the total luminosity from the protostar and its circumstellar disk if present. The bolometric luminosity of a source can then defined as $L_{\rm bol} = L_{\rm int} + L_{\rm ext}$, where the external luminosity comes from the heated protostellar envelope. It is estimated that $L_{\rm ext}$ contributes to $L_{\rm bol}$ on the order of 0.1 $L_\odot$ Dunham et al. (2008) developed a scaling law relating an embedded protostar's 70 μm flux to its internal luminosity $L_{\rm int}$.

4.3. *The S_{radio} and L_{bol} Relationship*

4.4. *Sources of Molecular Outflow*

The Serpens South embedded cluster occupies a region in projected proximity to the larger Aquila Rift complex, the W40 HII region and the Serpens Main molecular cloud. The Aquila Rift, as previously noted, is a local complex of dark molecular clouds extending several degrees, encompassing the Serpens Main molecular cloud, Serpens South and the W40 HII region (see Figure 1), which are the three main regions of star formation in the direction of the Aquila Rift (Eiroa et al. 2008).

5. CONCLUSIONS

REFERENCES

Anglada, G., Villuendas, E., Estalella, R., et al. 1998, AJ, 116, 2953 [1]

Beltrán, M. T., Estalella, R., Anglada, G., Rodríguez, L. F., & Torrelles, J. M. 2001, AJ, 121, 1556 [1]

Bertin, E., & Arnouts, S. 1996, A&AS, 117, 393 [3.1]

Bontemps, S., André, P., Könyves, V., et al. 2010, A&A, 518, L85 [1, 4.1]

Briggs, D. S. 1995, dissertation [1, 2, 2]

Clark, B. G. 1980, A&A, 89, 377 [2]

Curiel, S., Rodriguez, L. F., Bohigas, J., et al. 1989, Astrophysical Letters and Communications, 27, 299 [1]

Dunham, M. M., Crapsi, A., Evans, II, N. J., et al. 2008, ApJS, 179, 249 [4.2]

Dzib, S., Loinard, L., Mioduszewski, A. J., et al. 2011, in Revista Mexicana de Astronomia y Astrofisica Conference Series, Vol. 40, Revista Mexicana de Astronomia y Astrofisica Conference Series, 231–232 [1.1]

Eiroa, C., Djupvik, A. A., & Casali, M. M. 2008, The Serpens Molecular Cloud (Unpublished), 693 [4.4]

Eiroa, C., Torrelles, J. M., Curiel, S., & Djupvik, A. A. 2005, AJ, 130, 643 [1]

Fernández-López, M., Arce, H. G., Looney, L., et al. 2014, ApJ, 790, L19 [1]

Fomalont, E. B., Windhorst, R. A., Kristian, J. A., & Kellerman, K. I. 1991, AJ, 102, 1258 [3.1]

Friesen, R. K., Medeiros, L., Schnee, S., et al. 2013, MNRAS, 436, 1513 [1]

Gutermuth, R. A., Bourke, T. L., Allen, L. E., et al. 2008, ApJ, 673, L151 [1, 1.1, 3, 4.1]

Högbom, J. A. 1974, A&AS, 15, 417 [2]

Kirk, H., Myers, P. C., Bourke, T. L., et al. 2013, ApJ, 766, 115 [1]

Kuhn, M. A., Getman, K. V., Feigelson, E. D., et al. 2010, ApJ, 725, 2485 [1.1]

Maury, A. J., André, P., Men'shchikov, A., Könyves, V., & Bontemps, S. 2011, A&A, 535, A77 [1, 3.1, 3]

Nakamura, F., & Li, Z.-Y. 2014, ApJ, 783, 115 [1]

Nakamura, F., Sugitani, K., Shimajiri, Y., et al. 2011, ApJ, 737, 56 [1]

Reipurth, B., Rodríguez, L. F., & Chini, R. 1999, AJ, 118, 983 [1]

Rodríguez, L. F., Rodney, S. A., & Reipurth, B. 2010, AJ, 140, 968 [1, 1.1]

Schwab, F. R. 1984, AJ, 89, 1076 [2]

Shirley, Y. L., Claussen, M. J., Bourke, T. L., Young, C. H., & Blake, G. A. 2007, ApJ, 667, 329 [1, 3.1]

Straižys, V., Černis, K., & Bartašiūtė, S. 2003, A&A, 405, 585 [1.1]

Sugitani, K., Nakamura, F., Watanabe, M., et al. 2011, ApJ, 734, 63 [1]

Tanaka, T., Nakamura, F., Awazu, Y., et al. 2013, ApJ, 778, 34 [1]

Teixeira, G. D. C., Kumar, M. S. N., Bachiller, R., & Grave, J. M. C. 2012, A&A, 543, A51 [1]

APPENDIX

These are my edit notes for the paper.

– What does Rob say about SS distance?

– What paper should I quote for infrared source extraction photometry analysis?

– Do we have to worry about vibrational dust emission in our 4.1 cm data?